INTERNATIONAL JOURNAL FOR NUMERICAL METHODS IN FLUIDS, VOL. 2, 25–42 (1982)

CONSISTENT VS. REDUCED INTEGRATION PENALTY METHODS FOR INCOMPRESSIBLE MEDIA USING SEVERAL OLD AND NEW ELEMENTS

M. S. ENGELMAN AND R. L. SANI

CIRES/NOAA, Department of Chemical Engineering, University of Colorado, Boulder, Colorado 80309, U.S.A.

P. M. GRESHO

Lawrence Livermore National Laboratory, Livermore, California 94550, U.S.A.

M. BERCOVIER

School of Applied Science and Technology, The Hebrew University, Jerusalem, Israel

SUMMARY

The frequently used reduced integration method for solving incompressible flow problems 'a la penalty' is critically examined vis-a-vis the consistent penalty method. For the limited number of quadrilateral and hexahedral elements studied, it is shown that the former method is only equivalent to the latter in certain special cases. In the general case, the consistent penalty method is shown to be more accurate. Finally, we demonstrate significant advantages of a new element, employing biquadratic (2-D) or triquadratic (3-D) velocity and *linear* pressure over that using the same velocity but employing bilinear (2-D) or trilinear (3-D) pressure approximation.

KEY WORDS Penalty Method Incompressible Flow Reduced Quadrature Finite Elements

1. INTRODUCTION

The majority of the recent finite element literature on the discretization of the incompressible Navier-Stokes equations, in primitive variable formulation, deals with the application of Galerkin's technique utilizing mixed interpolation (e.g. Gartling *et al.*[1]) or a penalty formulation (e.g. Hughes *et al.*[2]), the latter of which results in the replacement of the solenoidal velocity field constraint by $\nabla \cdot \mathbf{u} = -\lambda^{-1}p$ where $\lambda \gg 1$ is the penalty parameter. As shown by Sani *et al.*,[3,4] these two approaches have many similarities when viewed as a consistent application of Galerkin's technique to the appropriate continuum equations. However, essentially all of the investigations using the penalty approach have made use of selective reduced integration in order to effectively implement the technique. Since such reduced integration is now widely used to simulate complex flow phenomena in irregular geometries, both theoretical investigations and numerical experiments of the two approaches are desirable. Numerous investigators—Bercovier,[5] Malkus and Hughes,[6] Bercovier and Engelman,[7] Oden,[8] Song, *et al.*,[9] Malkus,[10] Johnson and Pitkaranta[11]—have provided insight into both the theoretical and numerical aspects of the problem. Herein we focus, firstly, on the question of the equivalence of the reduced integration and consistent finite element penalty method for the quadrilateral family of elements. We will show that the two methods are

0271-2091/82/010025-18$01.80

Received 13 April 1981
Revised 15 June 1981

generally *not* equivalent and, in fact, that reduced integration can generate less accurate results on isoparametric meshes. We also provide some assessment of the performance of various elements in two and three spatial dimensions, including the new quadratic velocity–linear pressure element mentioned in Sani *et al.*[3,4] While the examples presented are taken from fluid mechanics, the general conclusions apply equally to incompressible solid mechanics (see Bercovier *et al.*[12]). The body of the text will concentrate on the practical aspects of the two formulations; however, we also present, in an appendix, a more detailed mathematical analysis.

2 PENALTY MATRIX FORMULATION

Since the pressure formulation using a penalty approach is identical no matter whether the transient or steady, Navier–Stokes or Stokes, Newtonian or non-Newtonian equations of incompressible fluid flow are considered, the setting for our discussion will be the simpler equations of stationary Stokes flow (or, equivalently, the equations of linear isotropic incompressible elasticity):

$$\nabla \cdot \tau = \mathbf{f} \tag{1a}$$

$$\nabla \cdot \mathbf{u} = 0 \tag{1b}$$

where $\tau_{ij} = -p\delta_{ij} + 2\mu\varepsilon_{ij}$ is the stress tensor, $\mathbf{u}$ the Eulerian fluid velocity, p the pressure, μ the viscosity (constant) of the fluid and ε_{ij} the strain rate tensor given by

$$\varepsilon_{ij} = \tfrac{1}{2}(u_{i,j} + u_{j,i}) \tag{1c}$$

The weak variational or Galerkin formulation of problem (1) is:

Given appropriate velocity and pressure spaces V and Q respectively, find $(\mathbf{u}, p) \in V \times Q$ such that

$$a(\mathbf{u}, \mathbf{v}) - (p, \nabla \cdot \mathbf{v}) = (f, \mathbf{v}) \tag{2a}$$

$$(\nabla \cdot \mathbf{u}, q) = 0 \tag{2b}$$

for all $\mathbf{v} \in V$ and $q \in Q$. $(\cdot, \cdot)$ is the inner product

$$(\mathbf{u}, \mathbf{v}) = \int_V u_i v_i \, \mathrm{d}V$$

and

$$a(\mathbf{u}, \mathbf{v}) = 2\mu \int_V \varepsilon_{ij} v_{i,j} \, \mathrm{d}V$$

The finite element equations are obtained by considering the discretized approximation of (2):

Let V^h and Q^h be finite dimensional subspaces of V and Q respectively; then we seek $(\mathbf{u}_h, p_h) \in V^h \times Q^h$ such that

$$a(\mathbf{u}_h, \mathbf{v}_h) - (p_h \nabla_h \cdot \mathbf{v}_h) = (\mathbf{f}, \mathbf{v}_h) \tag{3a}$$

$$(\nabla_h \cdot \mathbf{u}_h, q_h) = 0 \tag{3b}$$

for all $\mathbf{v}_h \in V^h$ and $q_h \in Q^h$, where ∇_h is the linear operator (weak divergence operator) defined by

$$\nabla_h : V^h \to Q^h; (\nabla \cdot \mathbf{v}_h, q_h) = (\nabla_h \cdot \mathbf{v}_h, q_h) \quad \text{for all} \quad (\mathbf{v}_h, q_h) \in V^h \times Q^h. \tag{3c}$$

The definition of ∇_h can also be recast in the more succinct and oftentimes more suggestive form,

$$\nabla_h \cdot \mathbf{v}_h \equiv P_h(\nabla \cdot \mathbf{v}_h). \tag{3d}$$

where P_h is the projection operator from $V^h \to Q^h$ which is consistent with equation (3c). In general, $\nabla_h \cdot \mathbf{v}_h$ is different from $\nabla \cdot \mathbf{v}_h$, and in fact, only if $\nabla \cdot \mathbf{v}_h \in Q^h$ for *any* $\mathbf{v}_h \in V^h$ are the two equal.

The penalty function formulation of problem (3) replaces equation (3b) by the equation

$$(\nabla_h \cdot \mathbf{u}_h, q_h) = -\frac{1}{\lambda}(p_h, q_h) \tag{4}$$

where λ, a large number, is called the penalty parameter.

Thus the discretized penalty problem is:
Find $(\mathbf{u}_h^\lambda, p_h^\lambda) \in V^h \times Q^h$ satisfying

$$a(\mathbf{u}_h^\lambda, \mathbf{v}_h) - (p_h^\lambda, \nabla_h \cdot \mathbf{v}_h) = (\mathbf{f}, \mathbf{v}_h) \tag{5a}$$

$$(\nabla_h \cdot \mathbf{u}_h^\lambda, q_h) = -\frac{1}{\lambda}(p_h^\lambda, q_h) \tag{5b}$$

for all $\mathbf{v}_h \in V^h$ and $q_h \in Q^h$.

While the pressure portion, p_h, of the solution of problem (3) may be non-unique owing to contamination by spurious pressure modes, the corresponding pressure, p_h^λ, from problem (5), which satisfies

$$p_h^\lambda = -\lambda \nabla_h \cdot \mathbf{u}_h^\lambda, \tag{6}$$

is free of this non-uniqueness.[3,4]

Thus choosing q_h such that $q_h = \nabla_h \cdot \mathbf{v}_h$, or, what is equivalent—inserting (6) into (5a)—equation (5b) can be used to eliminate the pressure unknown p_h^λ from equation (5a) so that problem (5) reduces to the following equivalent form:
Find $\mathbf{u}_h^\lambda \in V^h$ such that

$$a(\mathbf{u}_h^\lambda, \mathbf{v}_h) + \lambda(\nabla_h \cdot \mathbf{u}_h^\lambda, \nabla_h \cdot \mathbf{v}_h) = (\mathbf{f}, \mathbf{v}_h) \tag{7a}$$

for all $\mathbf{v}_h \in V^h$.

The velocity solution from equation (7a) will be identical to that from equations (5a, b) and the pressure recovered via equation (6) will also agree with that from equations (5a, b). Note that equation (7a) can also be written as

$$a(\mathbf{u}_h^\lambda, \mathbf{v}_h) + \lambda(P_h(\nabla \cdot \mathbf{u}_h^\lambda), P_h(\nabla \cdot \mathbf{v}_h)) = (\mathbf{f}, \mathbf{v}_h). \tag{7b}$$

It is important to realize that equation (7a) or (7b) is different (in general) from

$$a(\mathbf{u}_h^\lambda, \mathbf{v}_h) + \lambda(\nabla \cdot \mathbf{u}_h^\lambda, \nabla \cdot \mathbf{v}_h) = (\mathbf{f}, \mathbf{v}_h) \tag{8}$$

which penalizes the *original* divergence constraint rather than the projected (weaker) constraint penalized in equation (7). It is well known, however, that in general, problem (8) is over-constrained, forcing practitioners to employ the selective reduced integration technique. On the other hand, it can be shown that sometimes problems (5) and (8) can generate results which are actually identical.

Hypothesis:

Given a V^h, select the nodal points for p_h^λ in the element to be the points associated with the *lowest* order Gaussian quadrature scheme which will give exact results for (i) $(\nabla \cdot \mathbf{u}_h^\lambda, q_h)$, and (ii) (p_h^k, q_h). (A higher order quadrature scheme will generate useless results even though problems (5) and (8) will still be equivalent.)

Then it follows from equations (6) and (3c) that at the Gaussian points α_i.

$$p_h^\lambda(\alpha_i) = -\lambda(\nabla_h \cdot \mathbf{u}_h^\lambda)(\alpha_i) = -\lambda(\nabla \cdot \mathbf{u}_h^\lambda)(\alpha_i) \tag{9}$$

and thus $\nabla_h \cdot \mathbf{u}_h^\lambda \in Q^h$ can be computed by using the values of $\nabla \cdot \mathbf{u}_h^\lambda$ at the Gaussian points. Finally, the equivalence follows by comparing equations (7) and (8) with the inner product terms, except $(\mathbf{f}, \mathbf{v}_h)$, evaluated by the above Gaussian quadrature scheme.

Although it is necessary to have an exact evaluation of the scalar product (p_h^λ, q_h) to obtain the above complete equivalence (i.e. equality), it is interesting that an inexact evaluation of (p_h^λ, q_h) appears to be viable, provided the resulting discrete operator is invertible and that the remainder of the hypothesis holds. (It can be interpreted in terms of a 'modified penalty parameter' and introduces an $O(1/\lambda)$ effect.) A few related numerical experiments will be discussed in Section 3 and Appendix I considers the general effect of inexact integration.

Additionally, it is noteworthy that Malkus and Hughes[6] have shown that the selective reduced integration form of (8) is *always* equivalent to a mixed penalty form (5) by requiring only (p_h^λ, q_h), $(\nabla_h \cdot \mathbf{u}_h^\lambda, q_h)$ and $(p_h^\lambda, \nabla_h \cdot \mathbf{v}_h)$ be evaluated by the *same* Gaussian quadrature scheme, which is not necessarily an exact evaluation when selective reduced integration is used. This result and the work of Oden and colleagues on the criteria for successful application of general reduced integration penalty (RIP) methods (see Reference 8 for a pertinent summary) are complementary to those presented herein.

The viability of the penalty formulation lies in the result[5]

$$\|\mathbf{u} - \mathbf{u}_h^\lambda\|_1 + \|p - p_h^\lambda\|_{L_2(\Omega)/R} \leqq \frac{C_1}{\lambda} + C_2(h). \tag{10}$$

where C_1 is a constant independent of λ and h, and $C_2(h)$ is a function of h which goes to zero as $h \to 0$. This states, for example, that the solution of the penalty problem (5) can be made as close as desired to the solution of (3) by a suitable choice of λ; in practice $\lambda \sim 10^6$–10^8. The validity of (10) and the behaviour of $C_2(h)$ are dependent on the space of functions chosen for the velocity and pressure and have been questioned by some (e.g. References 8, 9, 11).

If $\{\varphi_i; i = 1, n\}$ and $\{\psi_i; i = 1, m\}$ are sets of basis functions for the finite dimensional spaces V^h and Q^h respectively, then the global finite element equations are obtained by applying the approximations

$$\mathbf{u}_h^\lambda = \sum_{k=1}^{n} \varphi_k \mathbf{u}_k \tag{11a}$$

$$\mathbf{p}_h^\lambda = \sum_{k=1}^{m} \psi_k p_k \tag{11b}$$

at element level and summing over all elements. $\mathbf{u}_k$ and p_k are the unknown element 'nodal' values of velocity and pressure. Inserting (11) into equations (5) or (8) and summing over all the elements leads to the GFEM equations which, written in matrix form, are:

$$(\mathbf{K}_d + \lambda \mathbf{K}_p)\mathbf{U} = \mathbf{F} \tag{12}$$

where $\mathbf{K}_d$ is the viscous matrix, $\mathbf{K}_p$ the penalty matrix and $\mathbf{U}$ is the global vector of unknown nodal velocities.

We shall be concerned here with the construction of the matrix $\mathbf{K}_p$, which is different depending on whether equations (5) or equation (8) is used. In particular, conditions for the equivalence of the different constructions will be investigated.

First we define a number of matrices we shall use in the following analysis; all matrices are considered at element level. Let $\mathbf{U}$ and $\mathbf{P}$ denote the vectors of 'nodal' values for $\mathbf{u} \in V^h$ and $p \in Q^h$, then

$$(\nabla_h \cdot \mathbf{u}, p) \equiv \mathbf{U}^T \mathbf{C} \mathbf{P} \quad \text{for all} \quad \mathbf{u} \in V^h, p \in Q^h \tag{13a}$$

$$(\nabla \cdot \mathbf{u}, \nabla \cdot \mathbf{v}) \equiv \mathbf{U}^T \mathbf{B} \mathbf{V} \quad \text{for all} \quad \mathbf{u}, \mathbf{v} \in V^h \tag{13b}$$

$$(p, q) \equiv \mathbf{P}^T \mathbf{M} \mathbf{Q} \quad \text{for all} \quad p, q \in Q^h \tag{13c}$$

$\mathbf{M}$ is an $m \times m$ matrix, sometimes referred to as the pressure mass matrix on Q^h, $\mathbf{B}$ an $nN \times nN$ matrix and $\mathbf{C}$ and $nN \times m$ matrix, where $N = 2$ or 3 depending on the number of space dimensions of the problem.

The matrices $\mathbf{B}, \mathbf{C}$ and $\mathbf{M}$ in three dimensions are computed by

$$\mathbf{M} = (m_{ij})_{m \times m}; \qquad m_{ij} = \int_E \psi_i \psi_j \, dE; \qquad i, j = 1, m \tag{14a}$$

$$\mathbf{C} = \begin{bmatrix} c_{ij}^1 \\ c_{ij}^2 \\ c_{ij}^3 \end{bmatrix}_{3n \times m}; \qquad c_{ij}^k = \int_E \frac{\partial \varphi_i}{\partial x_k} \psi_j \, dE; \quad \begin{matrix} i = 1, n \\ j = 1, m \end{matrix} \tag{14b}$$

$$\mathbf{B} = \begin{bmatrix} b_{ij}^{11} & b_{ij}^{12} & b_{ij}^{13} \\ b_{ij}^{21} & b_{ij}^{22} & b_{ij}^{23} \\ b_{ij}^{31} & b_{ij}^{32} & b_{ij}^{33} \end{bmatrix}_{3n \times 3n}; \qquad b_{ij}^{kl} = \int_E \frac{\partial \varphi_i}{\partial x_k} \frac{\partial \varphi_j}{\partial x_l} \, dE; \quad i, j = 1, n \tag{14c}$$

In two-dimensional problems

$$\mathbf{C} = \begin{bmatrix} c_{ij}^1 \\ c_{ij}^2 \end{bmatrix}_{2n \times m}; \qquad \mathbf{B} = \begin{bmatrix} b_{ij}^{11} & b_{ij}^{12} \\ b_{ij}^{21} & b_{ij}^{22} \end{bmatrix}_{2n \times 2n}$$

Returning to the formulations (5) and (8) of the penalty GFEM we see that if equations (5) are used then

$$\mathbf{K}_p = \mathbf{C} \mathbf{M}^{-1} \mathbf{C}^T. \tag{15a}$$

Once $\mathbf{U}$ is obtained from equation (12), the pressure is calculated via

$$\mathbf{P} = -\lambda \mathbf{M}^{-1} \mathbf{C}^T \mathbf{U} \tag{15b}$$

which is the realization of equation (6). We shall refer to this as the consistent penalty method as first mentioned in References 3 and 4.

On the other hand if equation (8) is used to form $\mathbf{K}_p$, it is then simply

$$\mathbf{K}_p = \mathbf{B}. \tag{16a}$$

In this case, once $\mathbf{U}$ is obtained from equation (12) the pressure is usually recovered at the appropriate Gauss points,

$$p_h^\lambda(\alpha_i) = -\lambda (\nabla \cdot \mathbf{u}_h^\lambda)(\alpha_i). \tag{16b}$$

Reduced integration is used to evaluate **B** (which we thus refer to as the reduced integration method) since, if full quadrature were used, the approach [via (8) and (14c)] is illegal because the system would be, effectively, over-constrained: there would be more continuity constraints than velocities to satisfy them. This exact integration of **B** would be equivalent to a particularly untenable application of equal order interpolation for velocity and pressure. Note that in the reduced integration approach, the pressure basis functions ψ_i do not enter *explicitly* into the construction of the penalty matrix $\mathbf{K}_p$. We shall, in the following sections, show under which choices of the basis sets $\{\varphi_i\}$ and $\{\psi_i\}$ and under what conditions the matrices **B** and $\mathbf{CM}^{-1}\mathbf{C}^T$ are equivalent and the possible implications of this equivalence on the accuracy of the computed finite element solution.

In the ensuing discussion $\{\alpha_j: j=1, l\}$ will denote the co-ordinates of l-point Gaussian integration in an element and $\{w_j: j=1, l\}$ the corresponding weighting factors. **J** will denote the $N \times N$ Jacobian matrix of the transformation from a reference element $\hat{\mathbf{E}}$ to the element under consideration **E**, $|\mathbf{J}|$ its determinant and $\{\xi_k: k=1, N\}$ the natural co-ordinate system of the reference element. P_k will be the space of polynomials in N variables of degree $\leqq k$, and Q_k the space of polynomials in N variables of degree $\leqq k$ in *each* variable; where N is understood to be 2 or 3 depending on the context. $\{\mathbf{x}_j: j=1, r\}$ will denote the nodal co-ordinates of an r-node element.

Two-dimensional elements

(a) *Bilinear 4-node quadrilateral.* This is the simplest possible two-dimensional quadrilateral element ($\varphi_i \in Q_1$). The φ_i, being nodal basis functions have the property that $\varphi_i(\mathbf{x}_j) = \delta_{ij}$. The pressure basis functions are chosen to be of one order less in degree than the velocity basis functions, implying that ψ_i is constant over the element; i.e. $\psi_i = 1 \in Q_0$ (or equivalently P_0).

The **C** and **M** matrices are evaluated as

$$c_{ij}^k = \int_E \psi_j \frac{\partial \varphi_i}{\partial x_k} \, dE = \int_{\hat{E}} \psi_j \left[\sum_{L=1}^{N} \frac{\partial \varphi_i}{\partial \xi_L} \frac{\partial \xi_L}{\partial x_k} \right] |\mathbf{J}| \, d\hat{E} \tag{17a}$$

$$m_{ij} = \int_E \psi_i \psi_j \, dE = \int_{\hat{E}} \psi_i \psi_j \, |\mathbf{J}| \, d\hat{E} \tag{17b}$$

For this element, these integrals can be evaluated exactly using one-point Gaussian quadrature. Therefore, for the jth element,

$$c_{ij}^k = \frac{\partial \varphi_i}{\partial x_k}(\alpha_1) \, |\mathbf{J}(\alpha_1)| \, w_1,$$

$$m_{ij} = |\mathbf{J}(\alpha_1)| \, w_1 \delta_{ij},$$

and so

$$\mathbf{K}_p = \mathbf{CM}^{-1}\mathbf{C}^T = \begin{bmatrix} \dfrac{\partial \varphi_i}{\partial x_1}(\alpha_1) \dfrac{\partial \varphi_j}{\partial x_1}(\alpha_1) \, |\mathbf{J}(\alpha_1)| \, w_1 & \textit{symmetric} \\ \dfrac{\partial \varphi_i}{\partial x_1}(\alpha_1) \dfrac{\partial \varphi_i}{\partial x_2}(\alpha_1) \, |\mathbf{J}(\alpha_1)| \, w_1 & \dfrac{\partial \varphi_i}{\partial x_2}(\alpha_1) \dfrac{\partial \varphi_j}{\partial x_2}(\alpha_1) \, |\mathbf{J}(\alpha_1)| \, w_1 \end{bmatrix}$$

This matrix is exactly the **B** matrix evaluated using one-point Gaussian integration. Therefore for this element the consistent and reduced integration techniques are equivalent and result in the same penalty matrix $\mathbf{K}_p$.

(b) *Biquadratic 9-node quadrilateral.* For this element $\varphi_i \in Q_2$. The requirement that the order of the pressure basis functions ψ_i be less than that of the velocity basis functions allows three possible choices for the ψ_i; $\psi_i \in Q_0$, $\psi_i \in Q_1$ or $\psi_i \in P_1$. The choice $\psi_i \in Q_0$ is not considered herein and we first consider $\psi_i \in Q_1$, where the ψ_i are defined at the 2×2 points of Gaussian integration of the reference element, i.e. $\psi_i(\alpha_j) = \delta_{ij}$. Performing a similar analysis as for the bilinear quadrilateral reveals that the **B** matrix (now evaluated by 2×2 reduced integration) will be equivalent (equal) to the matrix $\mathbf{C}\mathbf{M}^{-1}\mathbf{C}^{\mathrm{T}}$ so long as 2×2 Gaussian integration computes the **C** and **M** matrices exactly. Examination of the integrals (17a, b) (see also Reference 13),, reveals that for a straight-sided element, 2×2 Gaussian integration is sufficient to evaluate (17a, b) exactly. In this case the mass matrix reduces to a diagonal matrix, rendering the computation of its inverse trivial, as for the 4-node element. However, if the element is fully isoparametric with curved sides, 3×3 Gaussian integration is required to evaluate the **C** and **M** matrices exactly and **M** is now a full 4×4 symmetric matrix. In this situation, the use of reduced integration will introduce an integration error into the computation of the penalty matrix $\mathbf{K}_p$ and subsequently an error into the computed velocity and pressure solutions (see also Appendix I).

Remark: Note that if 3×3 Gaussian integration is used to evaluate the **B** matrix, the result is equivalent to a consistent construction of $\mathbf{K}_p$ using $\psi_i \in Q_2$ defined at the 3×3 Gaussian integration points; i.e. both the velocity and pressure will be approximated quadratically. However, as mentioned earlier, such an approach leads to an overconstrained system.

The situation for $\psi_i \in P_1$ is more complex. It is no longer straightforward to find basis functions $\psi_i \in P_1$ with the desirable property $\psi_i(\alpha_j) = \delta_{ij}$ for some set $\{\alpha_j\colon\ j = 1, 3\}$ of integration points. There are two possible choices for the P_1 space; either on the reference element, i.e. $\{1, \xi_1, \xi_2\}$ or in the global co-ordinate system, i.e. $\{1, x_1, x_2\}$ and $p = a + bx_1 + cx_2$. We chose the latter because we know then that (10) can be shown to be satisfied (cf. Hecht[14]).

The pressure mass matrix **M** is now always a full symmetric 3×3 matrix given by

$$\mathbf{M} = \begin{pmatrix} \int_E \mathrm{d}E & & \textit{symm} \\ \int_E x\,\mathrm{d}E & \int_E x^2\,\mathrm{d}E & \\ \int_E \mathrm{y}\,\mathrm{d}E & \int_E xy\,\mathrm{d}E & \int_E \mathrm{y}^2\,\mathrm{d}E \end{pmatrix}$$

and the penalty matrix must be constructed by first computing its inverse $\mathbf{M}^{-1}$ and then forming the matrix product $\mathbf{C}\mathbf{M}^{-1}\mathbf{C}^{\mathrm{T}}$. A 3×3 Gaussian integration rule must be used to evaluate **C** and **M** for this element (see Appendix I).

One of the major advantages of the $p \in P_1$ over the $p \in Q_1$ formulation is the absence of the spurious checkerboard pressure mode.[4]

Three-dimensional elements

(a) *Trilinear 8-node isoparametric brick.* Similar to the 4-node quadrilateral, $\varphi_i \in Q_1$ and $\psi_i \in Q_0$, i.e. $\psi_i = 1$. In the reduced integration formulation, one-point Gaussian integration must be used again to evaluate the **B** matrix. This matrix will be equal to $\mathbf{C}\mathbf{M}^{-1}\mathbf{C}^{\mathrm{T}}$ so long as one-point integration computes the **C** and **M** matrices exactly. This occurs only if the element is a rectangular prism; otherwise it is erroneous. If the element is a general 3-D hexahedron, then $2\times2\times2$ Gaussian integration must be used to compute **C** and **M** exactly.

For such an element the consistent construction of $\mathbf{K}_p$ must be employed to obtain the error-free penalty matrix contribution.

(b) *Triquadratic 27-node isoparametric 'brick'*. The analysis for the 27-node brick is analogous to that of the 2-D 9-node quadrilateral; i.e. $\varphi_i \in Q_2$ and the pressure basis functions can be chosen in Q_1 or P_1. If $\psi_i \in Q_1$, examination of the integrals in the **C** and **M** matrices reveals that the reduced integration construction of $\mathbf{K}_p$, using $2\times2\times2$ Gaussian integration, is equivalent to the consistent construction only for rectangular prism elements. General straight-sided parallelepipeds require $3\times3\times3$ Gaussian integration to evaluate the **C** and **M** matrices exactly; while if a general curved-sided isoparametric brick is considered, $4\times4\times4$ integration is necessary for **C** to be computed without error. Note that once Gaussian integration of an order greater than 2 is used to compute the pressure mass matrix **M**, it is no longer diagonal but a full 8×8 symmetric matrix. To construct the penalty matrix for such a case, the 8×8 matrix **M** must be constructed, inverted and the product $\mathbf{CM}^{-1}\mathbf{C}^T$ formed, where **C** is an 81×8 matrix. As the operation counts in Appendix II testify, this is a costly operation.

For the $\psi_i \in P_1$ formulation the basis set, $\{1, x_1, x_2, x_3\}$ is used; i.e. $p = a + bx_1 + cx_2 + dx_3$. Again only the consistent construction is possible; however this construction is less expensive than that for $p \in Q_1$, since there are now only 4 basis functions for the pressure as compared to 8 for the $p \in Q_1$ formulation. This fact, together with the absence of spurious checkerboard pressure modes, makes it a very attractive element in principle. In the next section we demonstrate numerically that it is also more accurate than the $p \in Q_1$ element.

We have noted that for both the $p \in Q_1$ and the $p \in P_1$ consistent formulations, $4\times4\times4$ integration is required for curved isoparametric elements. In Appendix I it is shown that for these elements, $3\times3\times3$ Gaussian integration for the **C** matrix is actually sufficiently accurate because the error introduced by the integration rule is small relative to the approximation error for the element.

It is interesting to note (see Appendix II) that if, for the $p \in Q_1$ consistent construction, $3\times3\times3$ integration is used for the **C** matrix and $2\times2\times2$ instead of the required $3\times3\times3$ integration is employed to compute **M** (thus reducing it to a diagonal matrix), the savings in operations is only on the order of 10 per cent.

3. NUMERICAL EXPERIMENTS

A series of numerical experiments was undertaken to verify the behaviour predicted by the preceding theory. Since we wish to estimate the error resulting from the use of the different formulations, it is necessary to simulate flows which have non-trival analytic velocity and pressure solutions. For the problems studied the measure of the error in the velocity and pressure solutions was taken to be

$$\text{relative RMS error in velocity} = \left[\frac{\sum_i \|\mathbf{u}_i^e - \mathbf{u}_i^c\|^2}{\sum_i \|\mathbf{u}_i^e\|^2}\right]^{1/2}$$

$$\text{relative RMS error in pressure} = \left[\frac{\sum_i (p_i^e - p_i^c)^2}{\sum_i (p_i^e)^2}\right]^{1/2}$$

where $\|\mathbf{u}\| = (\sum_{i=1}^{N} u_i^2)^{1/2}$ is the Euclidean norm and $\mathbf{u}_i^e, \mathbf{u}_i^c$ are, respectively, the exact and computed velocity solutions at node i. Similarly p_i^e, p_i^c are the exact and computed pressure solutions at the centroid of element i. Centroid pressures are used in the experiments to

compare the different penalty matrix constructions (where appropriate) so as to eliminate the contribution of the spurious pressure mode to the computed pressures.

Two-dimensional experiments

Two problems were chosen for study; one linear (body force) and one non-linear (colliding flow).

(a) *Body Force problem—Stokes.* A body force with components

$$F_x(x, y) = F(x, y) + y - \tfrac{1}{2}$$

and

$$F_y(x, y) = -F(y, x) + x - \tfrac{1}{2},$$

where

$$F(x, y) = 256[6x^2(x-1)^2(2y-1) + y(y-1)(2y-1)(12x^2 - 12x + 2)],$$

is applied to a fluid contained within a unit square with $\mathbf{u} = \mathbf{0}$ on the entire boundary. The exact solution is

$$u_x(x, y) = -256x^2(x-1)^2y(y-1)(2y-1).$$
$$u_y(x, y) = -u_x(y, x),$$
$$p = (x - \tfrac{1}{2})(y - \tfrac{1}{2}).$$

Due to the symmetrical properties of the problem only the lower left hand quadrant of the region was modelled.

(b) *Colliding flow problem—Navier Stokes.* In this example, fluid flows from $+y_\infty$ and $-y_\infty$ to collide at $y = 0$. The solution over the entire X–Y plane is

$$u_x = Cx$$
$$u_y = -Cy$$
$$p = -\frac{C}{2}\rho(x^2 + y^2)$$

The region $0 \leqq x \leqq 1, 0 \leqq y \leqq 1$ was modelled with symmetry planes (zero normal velocity and tangential stress) prescribed along $x = 0$ and $y = 0$ and the exact solution along $x = 1$ and $y = 1$. The parameters used were $C = 4$, $\rho = 1$ and $\mu = 0{\cdot}0667$.

The approximate solution to each problem was obtained using both the reduced integration and the consistent construction of the penalty matrix for $p \in Q_1$ and $p \in P_1$ on three different meshes. The meshes were: a regular 6×6 mesh of 9-node squares, a 6×6 mesh of irregular quadrilaterals, and a 6×6 mesh of curved isoparametric elements. The isoparametric mesh was generated by moving each midside node inwards or outwards a distance of 5 per cent of the element width. The latter two meshes are shown in Figures 1(a) and (b).

The results of the simulations of the body force problem are presented in Table I. They are in complete agreement with the theoretical predictions; that is, on both the regular and distorted quadrilateral meshes both the reduced and consistent constructions of the penalty matrices give essentially identical solution errors. It is only on the curved isoparametric meshes that the differences between the reduced and consistent formulations manifest themselves. Here we see a large error in the pressure solution when reduced integration is used which decreases markedly when a consistent construction is employed.

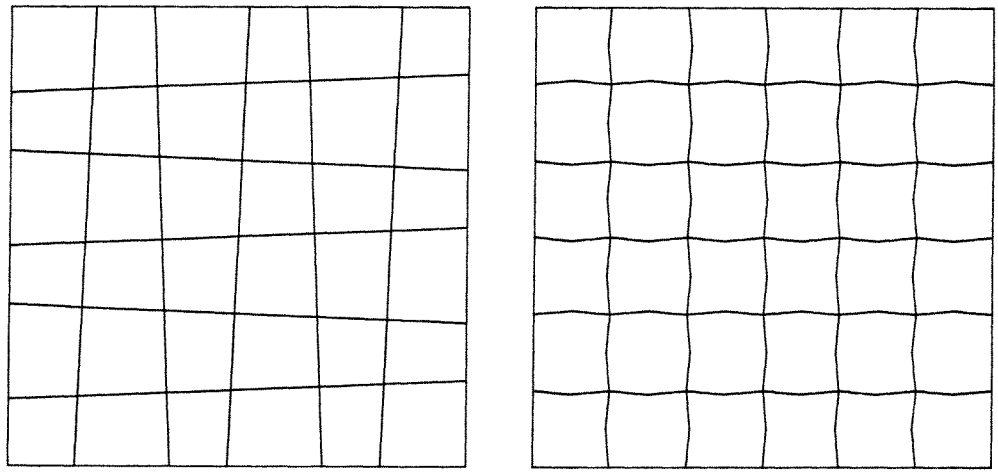

(a) (b)

Figure 1. Mesh of 9-node distorted quadrilaterals.

Table I. 2-D body force problem

Mesh	Pressure formulation	Correct centroids Rel. error velocity	Correct centroids Rel. error pressure	Displaced centroids Rel. error velocity	Displaced centroids Rel. error pressure
Rectangles	Reduced integration $p \in Q_1$	0·00004732	0·002699		
	Consistent $p \in Q_1$	0·00004734	0·002700		
	Consistent $p \in P_1$	0·00004701	0·002689		
Distorted quadrilaterals	Reduced integration $p \in Q_1$	0·0001036	0·007469	0·0004461	0·03087
	Consistent $p \in Q_1$	0·0001036	0·007469	0·0003628	0·02848
	Consistent $p \in P_1$	0·0001046	0·006803	0·0003501	0·02468
Isoparametric elements	Reduced integration $p \in Q_1$	0·003259	0·2282	0·005338	0·4487
	Consistent $p \in Q_1$	0·001681	0·1231	0·002468	0·1455
	Consistent $p \in P_1$	0·0005244	0·1011	0·0005929	0·09821

A corollary of the theoretical predictions in Section 2 is that if the midside nodes, or the centroid node, of an element are perturbed from their 'natural' position, the reduced integration and consistent constructions of $\mathbf{K}_p$ should again differ. This is a ramification of the now fully isoparametric mapping from the reference to the actual element. To demonstrate this effect the centroids of the elements in the distorted quadrilateral mesh (Figure 1(a)) were moved about 5 per cent from their correct positions and the calculations repeated (midside nodes were properly located). The results are shown in Table I: whereas previously all three constructions of $\mathbf{K}_p$ yielded almost identical results, now the consistent formulations display rather less error than the reduced integration construction of $\mathbf{K}_p$. This effect is even more evident when the centroids of the elements in the isoparametric mesh are perturbed (see Table I). The effect of the midside and centroid node locations on the accuracy of the numerical results appears to have not been seriously addressed in the literature nor (perhaps) appreciated in numerical simulations.

The simulations for the colliding flow problem revealed similar behaviour. Only the results for the isoparametric mesh are reported in Table II, as the regular and quadrilateral meshes gave nearly identical errors for all three formulations.

Table II. 2-D colliding flow problem

Mesh	Pressure formulation	Rel. error velocity	Rel. error pressure
Isoparametric elements	Reduced integration $p \in Q_1$	0·05057	0·02384
	Consistent $p \in Q_1$	0·03185	0·02129
	Consistent $p \in P_1$	0·01876	0·01601

Three-dimensional experiments

The availability of non-trivial analytic velocity and pressure solutions to three-dimensional fluid flows is very limited. For our simulations we have generalized the body force problem utilized in the previous section to three dimensions:

A body force,

$$F_x(x, y, z) = F(x, y, z) + P(x, y, z)$$
$$F_y(x, y, z) = -\tfrac{1}{2}F(y, z, x) + P(y, z, x)$$
$$F_z(x, y, z) = -\tfrac{1}{2}F(z, x, y) + P(z, x, y)$$

where

$$F(x, y, z) = -8(2y-1)(2z-1)\{(6x^2-6x+1)y(y-1)z(z-1) + 3x^2[z(z-1)+y(y-1)]\}$$
$$P(x, y, z) = (y-\tfrac{1}{2})(z-\tfrac{1}{2})$$

is applied to a fluid contained within a three-dimensional unit box with $\mathbf{u} = \mathbf{0}$ on the entire boundary. The exact (Stokes) solution is

$$u_x(x, y, z) = 4x^2(x-1)^2y(y-1)(2y-1)z(z-1)(2z-1)$$
$$v_y(x, y, z) = -\tfrac{1}{2}u_x(y, z, x)$$
$$u_z(x, y, z) = -\tfrac{1}{2}u_x(z, x, y)$$
$$p = (x-\tfrac{1}{2})(y-\tfrac{1}{2})(z-\tfrac{1}{2})$$

Due to the symmetrical properties of the problem only the lower left hand quadrant of the box was modelled with zero tangential flow being specified on the three faces $x = \frac{1}{2}$, $y = \frac{1}{2}$ and $z = \frac{1}{2}$.

Only a limited number of simulations were performed to verify some of the predictions of the previous section. Two meshes were constructed: a $6 \times 6 \times 6$ regular mesh of 8-node bricks and a $6 \times 6 \times 6$ isoparametric mesh generated by randomly perturbing (by 5 per cent in the x, y and z directions) all internal nodes. Then using the same nodal points of these two meshes, a $3 \times 3 \times 3$ regular mesh and a $3 \times 3 \times 3$ isoparametric mesh comprising 27-node bricks were constructed. Simulations using the reduced and consistent $p \in Q_0$ formulations were performed on each of the 8-node brick meshes, and repeated using the reduced and consistent $p \in Q_1$ and consistent $p \in P_1$ constructions on each of the 27-node brick meshes. The results are tabulated in Tables III(a), (b). The results clearly confirm the theoretical predictions; the large errors in the pressure solutions on the isoparametric mesh are partly attributable to the coarseness of the mesh employed. Due to the presence of impure checkerboard pressure modes, we did not attempt to compute pressure errors on the isoparametric mesh of 8-node elements.

If both the two- and three-dimensional experiments are examined it is apparent that the $p \in P_1$ formulation consistently results in better, if not much better, solutions than either $p \in Q_1$ formulation. Also, in three dimensions, the $p \in P_1$ results are consistently much more accurate than those from the simpler 8-node element.

Table III. 3-D body force problem
(a) 8-node elements

Mesh	Pressure formulation	Rel. error velocity	Rel. error pressure
Rectangular prisms	Reduced integration $p \in Q_0$	0·03344	0·1480
	Consistent $p \in Q_0$	0·03344	0·1480
Hexahedrons	Reduced integration $p \in Q_0$	0·05231	CB modes
	Consistent $p \in Q_0$	0·04509	CB modes

(b) 27-node elements

Mesh	Pressure formulation	Rel. error velocity	Rel. error pressure
Rectangular prisms	Reduced integration $p \in Q_1$	0·0008196	0·03196
	Consistent $p \in Q_1$	0·0008196	0·03196
	Consistent $p \in P_1$	0·0007856	0·03242
Isoparametric hexahedrons	Reduced integration $p \in Q_1$	0·04765	1·149
	Consistent $p \in Q_1$	0·03549	0·9975
	Consistent $p \in P_1$	0·003975	0·1634

Variations on the mass matrix

During the course of our numerical simulations we also experimented with two simplifications for the pressure mass matrix **M** of the consistent $p \in Q_1$ formulation which result in the replacement of **M** by a diagonal matrix.

In the first of these $2\times2(\times2)$ Gaussian quadrature was used to compute **M**, and in the second (while not a generally recommended procedure) **M** was replaced by the identity matrix; in all cases the **C** matrix was evaluated sufficiently accurately. The results of our limited number of experiments indicated that the solutions are generally insensitive ($\sim O(1/\lambda)$) to the above approximations of **M** in accord with the expectations expressed in Section 2. These techniques could ostensibly be used to improve the cost-effectiveness of the $p \in Q_1$ element.

4. SUMMARY AND CONCLUSIONS

We have shown theoretically and demonstrated numerically that the consistent approach to the penalty method is, in general, the correct one and the reduced quadrature approach is only equivalent under certain conditions. When reduced quadrature is employed in other situations, the results may be significantly less accurate than those using the consistent method or its mixed interpolation counterpart.

Additionally, we have demonstrated, for the quadratic velocity elements that the new pressure approximation, $p \in P_1$, has sufficient advantages over the $p \in Q_1$ approximation to advocate its use. These are: (i) the absence of spurious pressure modes, (ii) higher accuracy, and (iii) greater cost-effectiveness. These advantages also apply to a mixed interpolation approach.

Finally, our numerical experiments also suggest that the construction of the penalty matrix is fairly insensitive to the form of the pressure mass matrix **M**; the **C** matrix is more important.

ACKNOWLEDGEMENTS

MSE and RLS would like to acknowledge support from the U.S. Army Research Office (Grant DAAG29–79–6–0045) and the National Science Foundation (Grant ATM 7923354). The authors are indebted to Dr. Michel Fortin whose review of the manuscript improved it significantly.

APPENDIX I

In this appendix we apply the work of Brezzi[15] to the mixed formulation of equation (3) in order to study the effect of the numerical integration used to compute the **C** and **M** matrices of (14a), (14b). Consider the following bilinear form on $V_h \times Q_h$

$$b(\mathbf{u}_h, p_h) = (\nabla_h \cdot \mathbf{u}_h, p_h) \tag{18}$$

and note that from the definition of equation (3c)

$$b(\mathbf{u}_h, p_h) = (\nabla \cdot \mathbf{u}_h, p_h) \tag{19}$$

In practice, the computation of (19) (i.e. the **C** matrix) requires a high order of integration. For instance, on a 3-D isoparametric 27-node brick, (19), with $p_h \in P_1(E)$ involves polynomials of degree seven. Thus, it is important to study the effect of numerical integration

error on (19), or more precisely on (14b). In a general setting this amounts to the introduction of a new bilinear form on $V_h \times Q_h : b^*(\mathbf{v}_h, q_h)$.

Recalling the original mixed formulation:

Find $(\mathbf{u}_h, p_h) \in V_h \times Q_h$ such that

$$\begin{aligned} a(\mathbf{u}_h, \mathbf{v}_h) + b(\mathbf{v}_h, p_h) &= (\mathbf{f}, \mathbf{v}_h) \\ b(\mathbf{u}_h, q_h) &= 0, \end{aligned} \tag{20}$$

we now have a new mixed variational problem:

Find $(u_h^*, p_h^*) \in V_h \times Q_h$ such that

$$\begin{aligned} a(\mathbf{u}_h^*, v_h) + b^*(\mathbf{v}_h, p_h^*) &= (\mathbf{f}, \mathbf{v}_h) \\ b^*(\mathbf{u}_h^*, q_h) &= 0. \end{aligned} \tag{21}$$

It is known[15] that if the hypothesis

$$\sup_{\mathbf{v}_h \in V_h - \{0\}} \frac{|b(\mathbf{v}_h, q_h)|}{\|\mathbf{v}_h\|_1} \geqq k \|q_h\|_0 \tag{22}$$

holds for every $q_h \in Q_h$, then (20) has a unique solution. The same is true for (21) if $b^*(\cdot, \cdot)$ satisfies (22). We now suppose that these two assumptions are satisfied. In general, (22) must be verified for each different element—as far as we know for the elements considered herein, this can only be done for the $Q_2 - P_1$ elements.

We introduce two measures of error

$$e_h^u(\mathbf{u}_h) = \sup_{\varphi \in Q_h - \{0\}} \frac{|b(\mathbf{u}_h, \varphi) - b^*(\mathbf{u}_h, \varphi)|}{\|\varphi\|_0} \tag{23a}$$

$$e_h^p(p_h) = \sup_{\mathbf{v} \in V_h - \{0\}} \frac{|b(\mathbf{v}, p_h) - b^*(\mathbf{v}, p_h)|}{\|\mathbf{v}\|_1} \tag{23b}$$

Then by a theorem of Brezzi[15] we have the error estimate:

$$\|\mathbf{u}_h - \mathbf{u}_h^*\|_1 + \|p_h - p_h^*\|_0 \leqq e_h^u(\mathbf{u}_h) + e_h^p(p_h) \tag{24}$$

Let E be an element and (w_i, α_i) be the weights and nodes of a quadrature rule over E, and set

$$b^*(\mathbf{v}_h, p_h)|_E = \sum_{i=1}^{l} \operatorname{div} \mathbf{v}_h(\alpha_i) p_h(\alpha_i) |\mathbf{J}(\alpha_i)| w_i; \tag{25}$$

then we can state the following lemma.

Lemma:

Suppose that on each element

$$\begin{aligned} b^*(\mathbf{v}, \varphi)|_E &= b(\mathbf{v}, \varphi)_E \quad \text{for all} \quad \mathbf{v} \in V_h \quad \text{and} \quad \varphi \in P_r \\ b^*(\mathbf{v}, \varphi)|_E &= b(\mathbf{v}, \varphi)_E \quad \text{for all} \quad \varphi \in Q_h \quad \text{and} \quad \mathbf{v} \in P_r \end{aligned}$$

where P_r is the space of polynomials of degree up to r in the global co-ordinates. Then

$$e_h^p \leqq C_1 h^{r+1} \quad \text{and} \quad e_h^u < C_2 h^{r+1} \tag{26}$$

where C_1, C_2 are constants independent of h.

Proof:

For any $\mathbf{v} \in V_h$ consider the linear from on Q_h:

$$L(\varphi) = b^*(\mathbf{v}, \varphi) - b(\mathbf{v}, \varphi)$$

By our assumptions $L(\varphi)$ is null on all elements for any $\varphi \in P_r$. Applying the Bramble–Hilbert lemma (cf. Ciarlet[16]) we obtain

$$|L(\varphi)| \leqq h^{r+1} \|\mathbf{v}\|_1 \|\varphi\|_0$$

The proof for the second inequality follows the same lines.

We can now apply these results to our $Q_2 - P_1$ element. Consider first the 2-D case; if we compute the c_{ij}^k of (14b) by means of a 2×2 Gaussian integration rule, we can apply our lemma with $r = 1$, but in order to establish (24) we must check that (22) holds. This is not the case here since the 2×2 rule does not define a unisolvent set for a Q_2 element.[16] Hence one must use a 3×3 rule—which is exact, for this element.

Next consider this element in the 3-D case. In order to apply our lemma with $r = 1$,we must use a $3 \times 3 \times 3$ Gaussian integration rule. This rule is based on a unisolvent set so that (22) holds and so does (24). We thus see that by using a $3 \times 3 \times 3$ Gaussian integration rule we remain within the approximation error.

For the penalty method we must also consider the error in computing the matrix $\mathbf{M}$. Note that we can rewrite (5a), (5b) as:

$$a(\mathbf{u}_h^\lambda, \mathbf{v}_h) - (p_h^\lambda, \nabla_h \cdot \mathbf{v}_h) = (\mathbf{f}, \mathbf{v}_h) \tag{27a}$$

$$(\nabla_h \cdot \mathbf{u}_h, q_h) = -\frac{1}{\lambda} D(p_h^\lambda, q_h) \tag{27b}$$

wherein $D(\cdot, \cdot)$ is *any* continuous bilinear form on $Q_h \times Q_h$ such that $D(\varphi, \varphi)^{1/2}$ defines a norm equivalent to the L_2 norm on Q_h (independent of h). Equation (14a) is then modified accordingly and we obtain

$$m_{ij}^* = D(\varphi_i, \varphi_j)\,|_E \tag{28}$$

Equations (27a)(27b) introduce a penalty function which is *equivalent* to our original one. Now we define $D(\cdot, \cdot)$ by means of a quadrature rule on each element

$$D(\varphi_k, \varphi_j)_E = \sum_{i=1}^{l} \varphi_k(\alpha_i) \varphi_j(\alpha_i) |\mathbf{J}(\alpha_i)| \, w_i \tag{29}$$

All our results will be true provided (29) defines a norm equivalent to the L_2 norm. This again is true if $\{\alpha_i\}$ is a unisolvent set for the element. This means that it is sufficient to use a $3 \times 3 \times 3$ Gaussian integration rule to evaluate (29).

APPENDIX II

In this appendix we review the mechanics of the construction of the penalty matrix using the 3 different possible schemes (for quadratic velocity elements) and estimate the number of operations involved. In the operation counts only multiplications and divisions are considered to contribute.

Notation:

NDP = Number of element nodal points
NDF = Number of velocity degrees of freedom per element
NIP = Number of integration points
α_j = Gaussian integration points
$\mathbf{J}(\alpha_j)$ = Jacobian value at α_j
w_j = Gaussian integration weight
NBF = Number of basis functions for pressure
NDIM = Number of dimensions

For the operation counts it is assumed that: (i) the values of $\partial\varphi_i/\partial x$, $\partial\varphi_i/\partial y$, ψ_i and $|\mathbf{J}|$ at the integration points have previously been computed; (ii) symmetry is invoked when $\mathbf{K}_p$ is formed.

Reduced integration

$$\begin{pmatrix} k_{ij}^{11} & & symm \\ k_{ij}^{21} & k_{ij}^{22} & \\ k_{ij}^{31} & k_{ij}^{32} & k_{ij}^{33} \end{pmatrix}_{3\text{-}D} ; \mathbf{K}_p = \begin{pmatrix} k_{ij}^{11} & symm \\ k_{ij}^{21} & k_{ij}^{22} \end{pmatrix}_{2\text{-}D}$$

where

$$k_{ij}^{mn} = \sum_{l=1}^{NIP} \frac{\partial\varphi_i}{\partial x_m}(\alpha_l)\frac{\partial\varphi_j}{\partial x_n}(\alpha_l)\,|\mathbf{J}(\alpha_l)|\,w_l$$

$$\text{No. of operations} = \text{NIP} \times \left(1 + \text{NDF} + \frac{(\text{NDF}+1)\times\text{NDF}}{2}\right)$$

$$= 760 \text{ in 2-D}$$

$$= 27{,}224 \text{ in 3-D}$$

Consistent $p \in Q_1$ (*rectangular elements*)

(i) Form $\mathbf{C}$ where

$$\mathbf{C} = \begin{pmatrix} c_{ij}^1 \\ c_{ij}^2 \\ c_{ij}^3 \end{pmatrix}_{3\text{-}D} ; \qquad \mathbf{C} = \begin{pmatrix} c_{ij}^1 \\ c_{ij}^2 \end{pmatrix}_{2\text{-}D}$$

and

$$c_{ij}^k \equiv \sum_{l=1}^{NIP} \frac{\partial\varphi_i}{\partial x_k}(\alpha_l)\psi_j(\alpha_l)\,|\mathbf{J}(\alpha_l)|\,w_l$$

(ii) Form $\mathbf{M}^{-1} = (m_{ij}^{-1})$ where

$$m_{ii}^{-1} \frac{1}{|\mathbf{J}(\alpha_i)|\,w_i} \qquad m_{ij}^{-1} = 0 \quad \text{for} \quad i \neq j$$

(iii) Form the product $\mathbf{C}\mathbf{M}^{-1}\mathbf{C}^{T}$

$$\text{No. of operations} = \begin{cases} \text{NIP}\times\text{NBF}\times(1+\text{NDP}\times\text{NDIM}) & \text{—(i)} \\ +2\times\text{NBF} & \text{—(ii)} \\ +\text{NDF}\times\text{NBF}\times\left(1+\dfrac{\text{NDF}+1}{2}\right) & \text{—(iii)} \end{cases}$$

$$= 1448 \quad \text{in 2-D}$$

$$= 44{,}944 \text{ in 3-D}$$

Consistent $p \in P_1$ *and isoparametric* $p \in Q_1$

(i) Form $\mathbf{M} = (m_{ij})_{3\times 3}$

$$m_{ij} = \sum_{l=1}^{\text{NIP}} \psi_i(\alpha_l)\psi_j(\alpha_l)\,|\mathbf{J}(\alpha_l)|\,w_l$$

(ii) Invert $\mathbf{M}$ (direct construction of inverse)
(iii) Form $\mathbf{C}$—as for consistent $p \in Q_1$ above
(iv) Form the product $\mathbf{C}^{T}\mathbf{M}^{-1}\mathbf{C}$

$$\text{No. of operations} = \begin{cases} \text{NBF}\times\text{NIP}\times(\text{NBF}+3)/2 & \text{—(i)} \\ +384(\text{3-D}, p \in Q_1), +64(\text{3-}D, p \in P_1 \text{ and 2-D}, p \in Q_1), \\ +34(\text{2-D}, \text{p} \in \text{P}_1) & \text{—(ii)} \\ +\text{NIP}\times(\text{NDIM}+\text{NDP}\times\text{NBF}\times\text{NDIM}) & \text{—(iii)} \\ +\text{NDF}\times\text{NBF}\times\text{NBF}+\dfrac{\text{NDF}\times(\text{NDF}+1)}{2}\times\text{NBF} & \text{—(iv)} \end{cases}$$

$$\left.\begin{aligned} &= 1294 \text{ in 2-D} \\ &= 23{,}851 \text{ in 3-D} \end{aligned}\right\} \quad p \in P_1$$

$$\left.\begin{aligned} &= 1828 \text{ in 2-D} \\ &= 50{,}901 \text{ in 3-D} \end{aligned}\right\} \quad p \in Q_1$$

Note that, suprisingly, the $p \in P_1$ construction is actually the least expensive procedure in 3-D; even for rectangular elements.

REFERENCES

1. D. K. Gartling, R. E. Nickell and R. I. Tanner, 'A finite element convergence study for accelerating flow problems', *Int. J. num. Meth. Engng*, **1,** 73 (1973).
2. T. J. R. Hughes, W. K. Liu and A. Brooks, 'Review of finite element analysis of incompressible viscous flows by penalty function formulation', *J. Comp. Phys.*, **30,** 1 (1979).
3. R. L. Sani, P. M. Gresho, R. L. Lee and D. F. Griffiths, 'The cause and cure (?) of the spurious pressures generated by certain FEM solutions of the incompressible Navier–Stokes equations: Part 1', *Int. j. numer. methods fluids*, **1,** 17 (1981).
4. R. L. Sani, P. M. Gresho, R. L. Lee, D. F. Griffiths and M. S. Engelman, 'The cause and cure (?) of the spurious pressures generated by certain FEM solutions of the incompressible Navier–Stokes equations: Part 2', *Int. j. numer. methods fluids*, **1,** 171 (1981).
5. M. Bercovier, 'Perturbation of mixed variational problems. Application to mixed finite element methods', *RAIRO Analyse Numerique*, **12,** 211 (1978).

6. D. S. Malkus and T. J. R. Hughes, 'Mixed finite element methods—reduced and selective integration techniques: a unification of concepts', *Comp. Meth. Appl. Mech. Eng.*, **15,** 63 (1978).
7. M. Bercovier and M. S. Engelman. 'A finite element for the numerical solution of viscous incompressible flows, *J. Comp. Phys.*, **30,** 181 (1979).
8. J. T. Oden, 'RIP-methods for Stokesian flows', *TICOM Report 80–11*, Texas Institute for Computational Mechanics, University of Texas at Austin, August (1980).
9. Y. J. Song, J. T. Oden and N. Kikuchi, 'Discrete LBB conditions for RIP-finite element methods', *TICOM Report 80–7*, Texas Institute for Computational Mechanics, University of Texas at Austin, August (1980).
10. D. S. Malkus, 'Finite element displacement model valid for any value of the compressibility,' *Int. J. Solids Structures*, **12,** 731 (1976).
11. C. Johnson and J. Pitkaranta, 'Analysis of some mixed finite element methods related to reduced integration', *Report 80·02 R* (1980), Dept. of Computer Science, Chambers University of Technology, Sweden.
12. M. Bercovier, Y. Hasbani, Y. Gilon and K-J. Bathe, 'On a finite element procedure for nonlinear incompressible elasticity', *Symp. Hybrid and Mixed Finite Elements*, Georgia Institute of Technology, April (1981).
13. J. M. Leone, P. M. Gresho, S. T. Chan and R. L. Lee. 'A note on the accuracy of Gauss–Legendre quadrature in the finite element method'. *Int. J. num. Meth. Engng*, **14,** 769 (1979).
14. F. Hecht, 'Divergence free finite elements for incompressible fluid flows', in preparation.
15. F. Brezzi, 'On the existence, uniqueness and approximation of saddle point problems arising from Lagrange multipliers', *RAIRO*, R.2 Aout, 129 (1974).
16. P. G. Ciarlet, *The Finite Element Method for Elliptic Problems*, North-Holland, Amsterdam, 1978.